Transition state spectroscopy of the I + HI reaction in clusters: Photoelectron spectroscopy of $IHI^- \cdot Ar_n$ ($n = 1$–15)

Zhuan Liu,[ab] Harry Gómez[ab] and Daniel M. Neumark*[ab]

[a] *Department of Chemistry, University of California, Berkeley, California 94720, USA*
[b] *Chemical Sciences Division, Lawrence Berkeley National Laboratory, Berkeley, CA 94720, USA*

Received 14th November 2000
First published as an Advance Article on the web 4th June 2001

We have investigated effects of solvation on the transition state spectroscopy and dynamics of the I + HI reaction by measuring the anion photoelectron (PE) spectra of the clusters $IHI^- \cdot Ar_n$ ($n = 1$–5). Argon clustering results in a successive shift of the PE spectra to lower electron kinetic energies with increasing cluster size. It also leads to significant vibrational cooling in the PE spectra and facilitates the observation of features associated with symmetric stretch vibrations and hindered rotational motions of the transition state complex IHI. The shifts in electron binding energy suggest that the first six argon atoms form a ring around the waist of the IHI^- anion, just as in $I_2^- \cdot Ar_n$. The spacing of the antisymmetric stretch features evolves with cluster size and is attributed at least in part to perturbation of the IHI^- geometry in larger argon clusters. Intensities of features due to hindered rotation are enhanced for larger clusters, possibly due to solvent perturbation of the neutral transition state region.

Introduction

A central issue in chemical reaction dynamics is the characterization of the transition state in a chemical reaction. In the past two decades, a number of experimental techniques have been developed to study transition state spectroscopy and dynamics of gas phase chemical reactions.[1–6] Anion photodetachment is one of the most powerful of these techniques.[7] In these experiments, photodetachment of a stable anion is used to access the transition state region of a neutral bimolecular reaction. If the geometry of the anion is similar to that of the transition state for the chemical reaction of interest, the resulting PE spectrum will contain detailed information on the transition state, including vibrationally-resolved structure characteristic of the transition state. This technique has been used to study a number of fundamental bimolecular chemical reactions $X + HY \rightarrow XH + Y$ (X and Y are halogen atoms, Cl, Br and I),[8–11] $F + H_2 \rightarrow HF + H$,[12,13] and $OH + H_2 \rightarrow H_2O + H$.[14] In this paper we extend these studies in a new direction, and investigate the effects of solvation on transition state dynamics through PE spectroscopy of clustered transition state precursors.

The effect of solvation on the transition state is of considerable interest,[15–17] given that most chemical reactions occur in solution. PE spectroscopy of clustered transition state precursor anions, in which the anions are clustered to known numbers of solvating species, offers a means of observing how the step-by-step solvation of the transition state affects its spectroscopy and dynamics. Previously, the PE spectra of singly clustered transition state precursors,

This journal is © The Royal Society of Chemistry 2001

$IHI^- \cdot N_2O$,[18,19] $IHI^- \cdot Ar$, and $BrHI^- \cdot Ar$ were studied in our laboratory. In this paper we examine solvation effects in larger clusters by measuring the PE spectra of $IHI^- \cdot Ar_n$ ($n = 1$–15).

The I + HI reaction is a prototype system for anion photodetachment studies. Although it is a direct reaction, and the IHI complex formed by photodetachment is unbound, the PE spectrum of IHI^- shows clearly resolved vibrational structure as was first shown by Weaver *et al.*[8] They observed a well-resolved progression in the spectrum and assigned it to the ν_3 antisymmetric (H-atom) stretch vibration of the neutral IHI complex. Waller *et al.*[9] applied higher resolution anion zero electron kinetic energy (ZEKE) spectroscopy to IHI^-, revealing more closely spaced progressions that were assigned to the symmetric stretch and hindered rotor motions of the unbound IHI complex; the observation of the symmetric stretch progression represented the first experimental identification of the quasibound states responsible for reactive resonances in a chemical reaction. Recently, we studied the transition state spectrum of IHI by PE spectroscopy of the binary cluster $IHI^- \cdot Ar$.[20] Clustering to a single Ar atom significantly reduces the contribution of vibrational hot bands to the PE spectrum, leading to even more fine structure associated mainly with IHI hindered rotor states than was seen in the ZEKE spectrum.

It is of interest to see if this structure survives in the PE spectrum of larger clusters, and, if so, how its evolution with cluster size can be interpreted in terms of solvation effects. The study of larger clusters is also motivated by recent theoretical work by Lavender and McCoy,[21] who reported a theoretical investigation on the short-time transition state dynamics of $ClHCl(Ar)_n$. They found that hydrogen rotational motion was strongly perturbed by the presence of argon atoms, but the stretch vibrations were much less affected. In the simulated PE spectra of $ClHCl^- \cdot Ar_n$, the main features that correspond to the stretching mode remain unchanged, while weaker bands due to bending vibrations exhibit a small increase in intensity.

In the PE spectra of $IHI^- \cdot Ar_n$, we expect to see two possible clustering effects relevant to transition state dynamics. First, the molecular structure of the anion may be affected by the presence of argon atoms. An altered anion geometry will shift the Franck–Condon region of the neutral potential energy surface (PES) accessed by photodetachment, enabling one to probe a slightly different region of the PES near the transition state. Second, dynamics on the neutral PES may be perturbed by argon atoms, leading to changes in the PE spectrum similar to those predicted by Lavender and McCoy[21] that cannot be attributed to anion solvation effects. In the present work, we see strong evidence for the change of anion geometry in $IHI^- \cdot Ar_n$, manifested by changes in the spacings of the major features in the PE spectra, and possible evidence for the second effect in the form of enhanced hindered rotor progressions for the largest clusters.

Experimental

The negative ion time-of-flight (TOF) PE spectrometer employed in this study has been described in detail previously,[10,22] and only particulars relevant to the present results will be summarized here. Anion clusters are produced at the intersection of a pulsed molecular beam and a 1 keV, 300 μA electron beam. The molecular beam is formed from a gas mixture of 0.01–0.1% HI in argon carrier gas which is expanded through a piezoelectric valve (0.1 mm diameter orifice) operated at 20 Hz with a stagnation pressure of 40 psig. Anion clusters generated in the supersonic expansion are cooled internally and extracted perpendicularly to the expansion by a pulsed electric field. They are then accelerated to a beam energy of 2.5 keV and enter a linear reflectron TOF mass spectrometer. The extracted ions separate in time and space according to their mass-to-charge ratios and are detected at the end of the flight tube by a pair of 25 mm diameter chevron-mounted microchannel plates.

Photoelectrons are detached from the mass-selected ions by a laser pulse from a Nd : YAG laser operated at 20 Hz. The ion of interest is selectively photodetached by controlling the laser firing delay. In the present study the fourth harmonic (266 nm, 4.66 eV) of the Nd : YAG laser is used. PE energies are determined by time-of-flight measurements in a 1 m field-free flight tube. In all experiments reported here, the laser beam is plane polarized perpendicular to the direction of electron collection. The resolution of the apparatus is 8–10 meV for an electron kinetic energy (eKE) of 0.65 eV and degrades as $(eKE)^{3/2}$ at higher eKEs. The 266 nm photons generate very small background signals through the interaction of scattered light with metal surfaces. A background spectrum, collected using the same laser power used during data collection, is fitted to a

smooth function, which is scaled and subtracted from the acquired data. The measured spectra are calibrated using the known PE spectra of I^-, Cl^- and Br^-.

Results

Fig. 1 shows two representative mass spectra of the $IHI^- \cdot Ar_n$ clusters. The spectra were measured under conditions optimized for smaller (a) and larger (b) clusters. We have observed clusters with up to 20 argon atoms, but the signal for clusters with more than 15 argon atoms was too weak to measure their PE spectra. The $n = 6$ and 13 clusters are possible magic numbers since they are local maxima in the $IHI^- \cdot Ar_n$ progression. Other peaks in the spectra are due to clusters of the type $I^- \cdot Ar_n$ and $IHI^- \cdot (HI)_x \cdot Ar_n$ ($x = 1, 2$).

The PE spectra of IHI^- and $IHI^- \cdot Ar_n$ collected at 266 nm are shown in Fig. 2. In previous work,[8] the three large peaks comprising the main progression in the IHI^- spectrum were assigned to transitions to the $v'_3 = 0$, 2 and 4 antisymmetric stretch levels of the IHI complex. When one argon atom is clustered to IHI^-, the PE spectrum is shifted to lower kinetic energy by about 18 meV. The linewidths of the $IHI^- \cdot Ar$ spectrum are also narrower compared to that of the corresponding features of bare IHI^-. In addition to the main progression, several small features are observed in the $IHI^- \cdot Ar$ spectrum. These include two weak progressions: one superimposed on the $v'_3 = 0$ peak (progression A) and the other (progression B) lying between the $v'_3 = 2$ and 4 peaks. Progressions A and B have previously been assigned to transitions to hindered rotor IHI levels that correlate to the $I + HI(v = 0, j)$ and $I + HI(v = 1, j)$ scattering channels, respectively.[9,20] Additional small features superimposed on the $v'_3 = 4$ peak in the $IHI^- \cdot Ar$ spectrum were assigned to a symmetric stretch (v_1) progression.[9,20]

Fig. 2 shows that when more argon atoms are added to IHI^-, the spectra are successively shifted to lower eKEs, but the main features remain similar to the $IHI^- \cdot Ar$ spectrum. The relative intensities, widths and peak envelopes are almost constant with increasing cluster size for $IHI^- \cdot Ar_n$ ($n \geqslant 1$). The total shifts of the $v'_3 = 0$, 2, 4 peaks for different numbers of argon atoms are given in Table 1. These shifts are determined by horizontally moving the peak of interest to achieve best overlap of the corresponding feature of $IHI^- \cdot Ar$. The stepwise shift, *i.e.* the shift per added argon atom, is also given in Table 1 in parentheses. In those cases where the stepwise shift cannot be determined directly ($n = 9$, 11, 13 and 15), because the $n - 1$ spectra were not recorded, the stepwise shift is taken as half the value of the shift between n and $n - 2$.

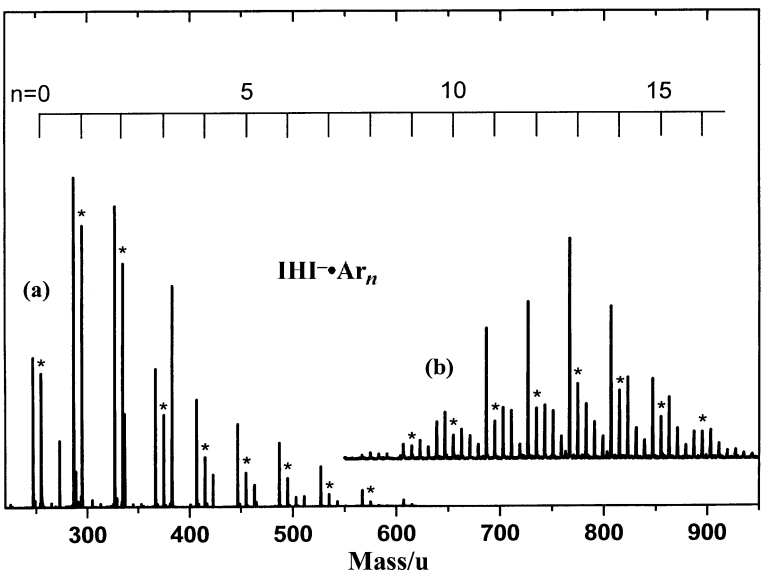

Fig. 1 Mass spectra of the $IHI^- \cdot Ar_n$ clusters with instrument optimized for low n (a) and high n (b). $IHI^- \cdot Ar_n$ clusters are marked with an asterisk (*).

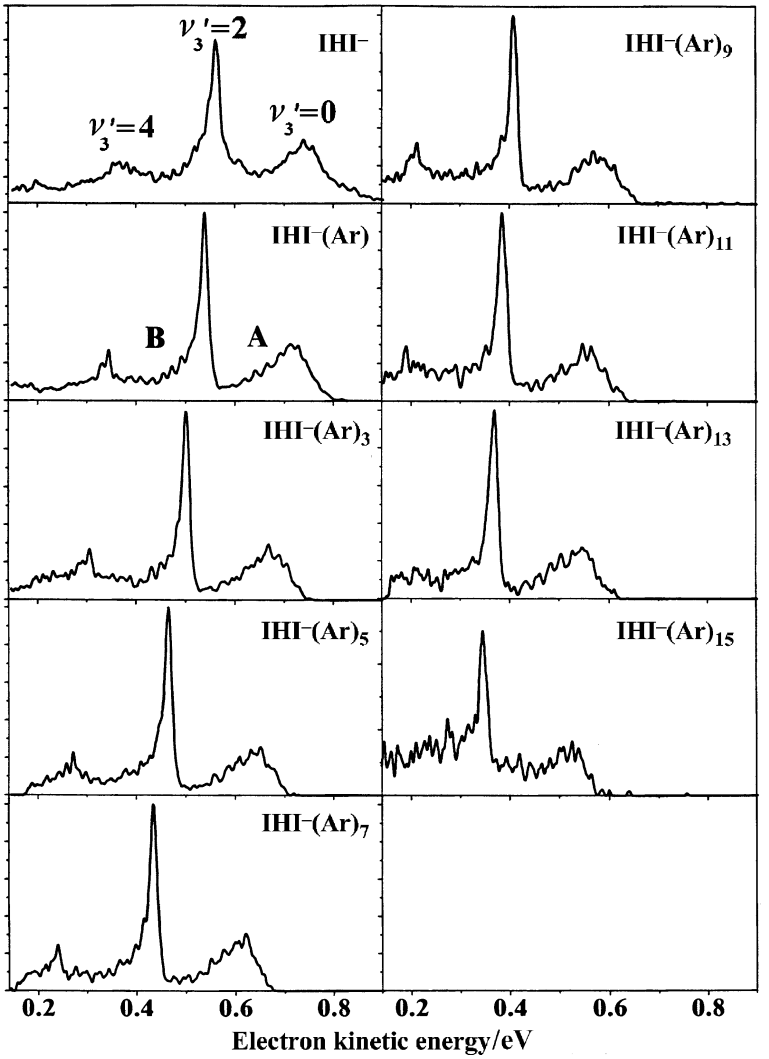

Fig. 2 Anion PE spectra of IHI^- and $IHI^- \cdot Ar_n$ ($n = 1,3,5,7,9,11,13,15$) recorded at a photon energy of 4.66 eV.

Table 1 shows that as the number of Ar atoms increases, the total shifts for the $v'_3 = 2$ and 4 peaks are the same, whereas the total shift for the $v'_3 = 0$ peak becomes systematically larger than for the $v'_3 = 2$ and 4 peaks. Hence, while the peak spacing between the $v'_3 = 2$ and 4 peaks remains constant, the spacing between the $v'_3 = 0$ and 2 peaks decreases as n increases (last column, Table 1) by as much as 12 meV. This effect is illustrated in Fig. 3, in which the $v'_3 = 0$ peak of the $IHI^- \cdot Ar$ is superimposed on the analogous feature in $IHI^- \cdot Ar_7$ (a) and $IHI^- \cdot Ar_{11}$ (b).

One of the most striking features of PE spectra of the larger clusters is that the weak features seen in the PE spectrum of $IHI^- \cdot Ar$ survive the addition of many more Ar atoms. In particular, progression A is visible in all the spectra up to $n = 15$. The spacing between the peaks comprising this progression does not change noticeably with cluster size, as can be seen by comparing the superimposed $v'_3 = 0$ peaks in Fig. 3. However, the intensity of this progression does vary; it appears to be slightly more intense and better-resolved for the three largest clusters ($n = 11,13,15$) in Fig. 2 than for the smaller clusters.

Fig. 4 shows the 266 nm PE spectra of $IHI^- \cdot Ar_n$ ($n = 1,3,5,7,9,11,13$) in the eKE between 0.8 and 1.6 eV, *i.e.* in a higher eKE range than the PE spectra in Fig. 2. All of these clustered IHI^-

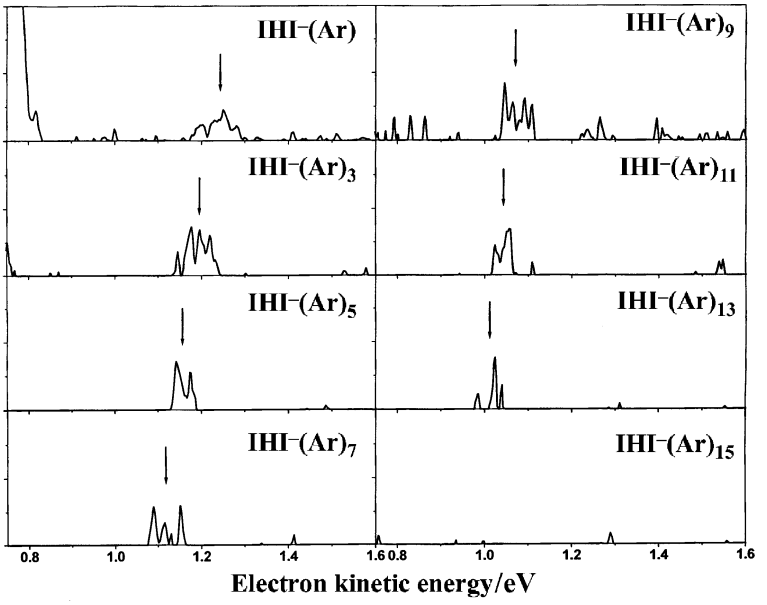

Fig. 4 Anion PE spectra of $IHI^- \cdot Ar_n$ (n = 1,3,5,7,9,11,13,15) at higher eKEs (0.8–1.6 eV).

spectra show a very weak feature around 1.0–1.3 eV that is not present in the bare IHI^- spectrum. These features, which are about 100 times weaker than the $v'_3 = 0$ peaks, shift to lower eKE when more argon atoms are added. The estimated center of each peak is indicated by the arrows in Fig. 4 and listed in Table 2. The apparent structure on some of the peaks represents noise due to counting statistics.

Discussion

In the following sections, the results are treated in more detail by considering the solvation effects of argon clusters on both the anion and the neutral transition state complex. We first consider the energetic information obtained from the spectral shifts and then discuss the change in peak spacing induced by Ar clustering, an effect we believe is largely due to perturbed anion geometries in the clusters. Solvation effects on the neutral transition state dynamics will be discussed in Section C and the possible carrier for the weak peaks at high eKE in Section D.

A. Energetics

As illustrated in Fig. 2, the PE spectra of $IHI^- \cdot Ar_n$ are successively shifted to lower electron kinetic energies with increasing cluster size. This phenomenon has been seen in several PE spectroscopy studies of anion clusters.[22–25] It is the result of differing interaction strengths of the solvent with the anion and neutral. Argon atoms bind to the IHI^- anion through the charge—induced dipole interaction, whereas binding to the neutral complex is from the much weaker Van der Waals interaction. As a consequence, each additional argon atom stabilizes the anion more than the neutral complex, leading to a shift of the PE spectrum toward lower eKE.

For each solvation step, *i.e.* the addition of one Ar atom to $IHI^- \cdot Ar_{n-1}$, the spectral shift is given by

$$\Delta E_{solv}(n) = E_{solv}(IHI^- \cdot Ar_n) - E_{solv}(IHI \cdot Ar_n) \quad (1)$$

where $E_{solv}(IHI^- \cdot Ar_n)$ and $E_{solv}(IHI \cdot Ar_n)$ are the stepwise solvation energies, defined as the dissociation energies for the loss of one argon atom from $IHI^- \cdot Ar_n$ and $IHI \cdot Ar_n$, respectively. The

total shift, $\Delta E_{\mathrm{solv,\,t}}(n)$, of the PE spectrum of $IHI^- \cdot Ar_n$ is the sum of the stepwise shifts. These shifts can be determined for each major feature in the PE spectra as discussed in the Results section and tabulated in Table 1. The $IHI^- \cdot Ar_n$ clusters are unique among anion clusters studied by PE spectroscopy so far in that not all the vibrational features shift the same amount upon solvation. Table 1 shows that the total shifts for $v'_3 = 2$ and 4 are essentially identical, while the shift for $v'_3 = 0$ is larger for each step. The origin of this effect is discussed in detail in Section B.

The total shifts for the $v'_3 = 2$ peaks are nearly linear in the region between $n = 0$ and 6; the shift per atom remains approximately constant at 18–20 meV from $n = 0$ to 6. For $n > 6$, the shift per atom becomes significantly smaller ($\sim$13 meV). To visualize this effect more clearly, the total shift, $\Delta E_{\mathrm{solv,\,t}}(n)$, is plotted against the cluster size for $v'_3 = 2$ in Fig. 5. The data from $n = 0$ to 6 are nicely fit by a straight line, while the best fit straight line from $n = 7$ to 15 clearly has a smaller slope. A similar trend is seen for the $v'_3 = 0$ peaks, although their shifts are determined less precisely because the peaks are broader.

The trends in the $v'_3 = 2$ peak shifts can be seen more clearly in Fig. 6, where the stepwise shifts $\Delta E_{\mathrm{solv}}(n)$ are plotted and compared with those obtained for $I_2^- \cdot Ar_n$ clusters in a similar PE spectroscopy study by Asmis *et al.*[22] Generally the trends in stepwise shifts for both $IHI^- \cdot Ar_n$ and $I_2^- \cdot Ar_n$ are strikingly similar. The stepwise shifts for both $IHI^- \cdot Ar_n$ and $I_2^- \cdot Ar_n$ are almost constant for the first six argon atoms with average values of 18 and 22 meV, respectively. After $n = 6$ they drop significantly to a similar average value of about 13 meV. This significant jump from $n = 6$ to 7 is a manifestation of the change in the slope in Fig. 5. In addition, there is a dip in the $I_2^- \cdot Ar_n$ plot around $n = 11$–13 that is also seen in the $IHI^- \cdot Ar_n$ data around $n = 12$–13.

Asmis *et al.*[22] have interpreted the considerable reduction of the stepwise shift between $n = 6$ and 7 as a change in binding site for the subsequent Ar atoms, a result consistent with molecular dynamics (MD) simulations on $I_2^-(Ar)_n$ clusters by Parson *et al.*[26] and Batista and Coker.[27] The first six argon atoms form a ring around the waist of the I–I bond, where they can interact with both I atoms. The sixth argon closes the ring, and subsequent argon atoms must bind to a single iodine atom, resulting in a weaker interaction because the excess negative charge is divided approximately equally between the two I atoms. The striking similarity in stepwise shifts between $IHI^- \cdot Ar_n$ and $I_2^- \cdot Ar_n$ suggests that similar effects are occurring in $IHI^- \cdot Ar_n$ clusters. The interpretation of our results in terms of the first several Ar atoms forming a ring is consistent with the calculations of Lavender and McCoy,[21] who calculated the minimum energy structure of $ClHCl^- \cdot Ar_n$ using a model potential. They found that the first five argon atoms cluster to the

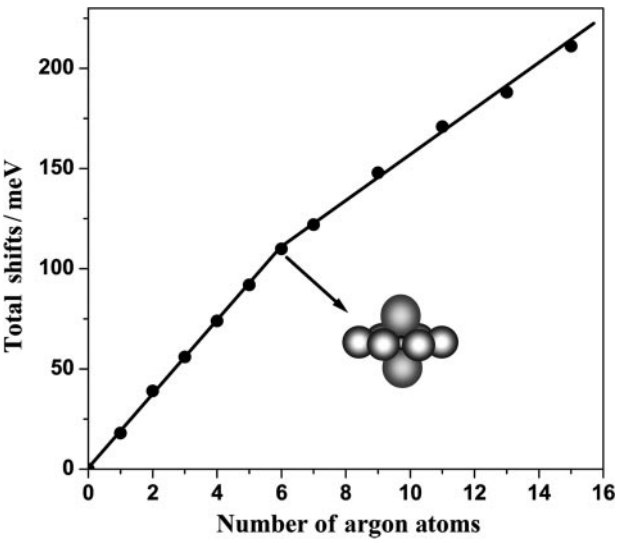

Fig. 5 The total spectral shift $\Delta E_{\mathrm{solv,\,t}}(n)$ for the $v'_3 = 2$ peak as a function of cluster size and the structure of the cluster at $n = 6$.

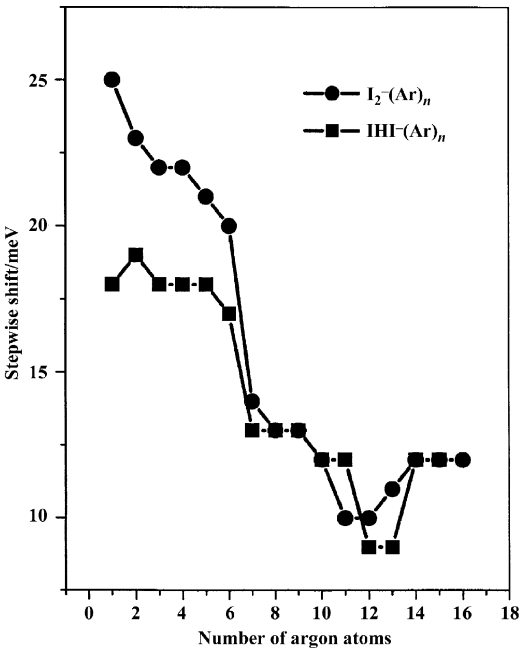

Fig. 6 The stepwise shift $\Delta E_{solv}(n)$ of the PE spectra of $IHI^- \cdot Ar_n$ and $I_2^- \cdot Ar_n$ as a function of cluster size.

$ClHCl^-$ anion in the plane that perpendicularly bisects the anion, forming a ring around the symmetry axis of the anion. Larger clusters were not considered in their calculations.

The MD simulations[26,27] of $I_2^- \cdot Ar_n$ indicate that once six argon atoms are added, the next seven Ar atoms cluster around one of the I atoms, inducing an asymmetrical distribution of the excess charge. This is followed by solvation of the other I atom until the first solvent shell is complete at $n = 20$. The comparison in Fig. 6 implies that a similar shell-filling pattern occurs in $IHI^- \cdot Ar_n$ clusters. It is particularly interesting to note that both data sets show a small dip at cluster sizes just below $n = 14$. In the light of the MD simulations, this observation suggests that for *both* types of clusters, the 13th argon completes the solvation of one I atom and the 14th binds to the "bare" I atom on the other side of the cluster. Since we have no data for $IHI^- \cdot Ar_n$ with $n > 15$, we cannot make any statements regarding the size of the first solvent shell for these species.

B. Change in peak spacings

We next consider the changes in peak spacing of the ν_3 features in the PE spectra as Ar atoms are added to the cluster. The vibrational progressions in an anion PE spectrum generally reflect the spacings between vibrational levels of the neutral, implying at first glance that this effect is from changes in the transition state vibrational spectrum due to Ar-induced perturbations in the neutral cluster. However, the situation is more subtle in transition state spectroscopy, because the neutral complex is in general unstable along one internal coordinate, and the vibrational frequencies of the modes perpendicular to this coordinate depend on its value. As a consequence, the spacing of the peaks in the PE spectrum, which reflects these perpendicular vibrational modes, can change if the location of the Franck–Condon region changes. Hence, perturbations of the IHI^- *anion* geometry induced by clustering with Ar atoms may be the origin of the observed changes in peak spacing.

The effect of anion geometry on the PE spectrum can be understood with reference to the three-dimensional vibrationally adiabatic curves shown in Fig. 7 for the I + HI reaction. These curves, as originally described by Kubach *et al.*,[28] show how I + HI(v, j) levels evolve adiabatically as the two I atoms are brought together and are obtained by solving the two-dimensional Schrod-

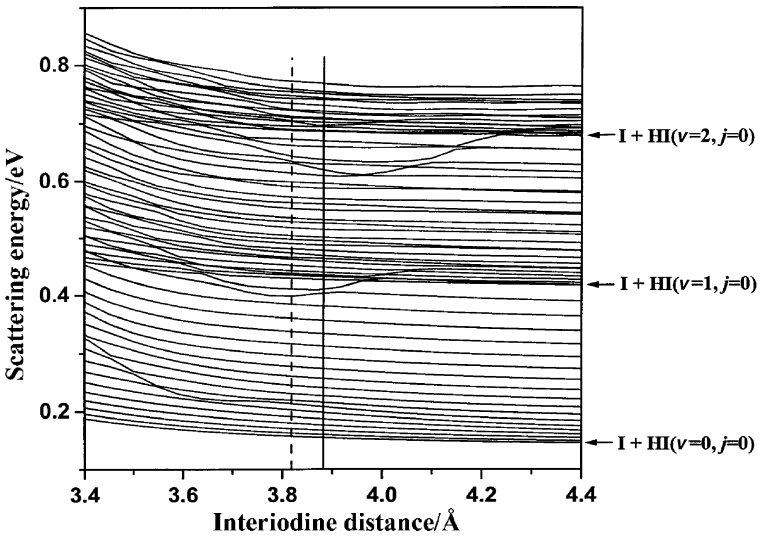

Fig. 7 Three-dimensional adiabatic curves calculated by Metz and Neumark *et al.*[29] for the I + HI reaction on the LEPS-C potential. Two vertical lines indicate the interiodine distances 3.88 Å (solid line) and 3.82 Å (dashed line).

inger equation for H-atom stretching and bending motion at fixed I–I bond distance. The curves in Fig. 7 were derived by Metz and Neumark *et al.*[29] from the LEPS-C model PES proposed by Schatz and Neumark *et al*[30] for the I + HI reaction. Only vibrational levels with *gerade* symmetry are shown, *i.e.* even v_3 levels, since transitions to odd v_3 levels of the complex from the anion ground state are forbidden. Hence asymptotic I + HI($v = n$) levels correlate to IHI($v_3 = 2n$) levels.

The IHI($v'_3 = 0$) curves are repulsive along the I–I coordinate. At large R_{I-I}, these curves correlate to various I + HI($v = 0, j$) rotational levels, and at smaller R_{I-I} they represent hindered rotor levels of the IHI complex. In contrast, the IHI $v'_3 = 2$ and 4 curves have wells that support IHI levels quasi-bound with respect to the symmetric stretch coordinate; these are the states responsible for I + HI reactive resonances. As shown in previous photodetachment experiments on IHI^-,[9,20] the $v'_3 = 0$ feature is due to a progression in IHI hindered rotor levels, while the $v'_3 = 2$ and 4 features are comprised of closely-spaced IHI symmetric stretch progressions, consistent with the adiabatic curves in Fig. 7.

We now consider the effect of changing the interiodine distance in the anion, as shown by the solid and dotted lines in Fig. 7. At shorter R_{I-I}, the separation between the repulsive IHI($v'_3 = 0$) and quasi-bound IHI levels with $v'_3 = 2$ and 4 is reduced, suggesting that if R_{I-I} is smaller in the larger $IHI^- \cdot Ar_n$ clusters, then the spacing between the corresponding features in the PE spectrum would follow the experimentally observed trend. This is considered more quantitatively by simulating the IHI^- PE spectrum at two values of R_{I-I} within the three-dimensional adiabatic approximation used by Metz and Neumark *et al.*[29] Fig. 8 shows simulated spectra at interiodine distances of 3.88 and 3.82 Å (the solid and dashed lines in Fig. 7); The larger value, 3.88 Å, is the estimated value of R_{I-I} in bare IHI^- based on our earlier PE spectra.[8] Fig. 8 shows that the energies of the $v'_3 = 2$ and 4 peaks are independent of R_{I-I}, although there are some changes in relative intensities due to Franck–Condon effects. However, each of the hindered rotor state transitions in $v'_3 = 0$ is shifted to lower electron kinetic energy as R_{I-I} is reduced. The overall contour of the $v'_3 = 0$ peak is therefore shifted closer to the $v'_3 = 2$ peak when the interiodine distance becomes smaller, giving a smaller peak spacing between $v'_3 = 0$ and 2 by about 4 meV. This result is comparable to what we observed in our $IHI^- \cdot Ar_n$ spectra, implying that a slight bond compression of the IHI^- occurs in the clusters.

This effect is consistent with the calculations by Lavender and McCoy[21] on $ClHCl^- \cdot Ar_n$ in which they found that the interhalogen distance decreased by 0.005 Å from $n = 0$ to 5. In related experimental work, Zanni *et al.*,[31] observed a blue shift in the I_2^- vibrational frequency in

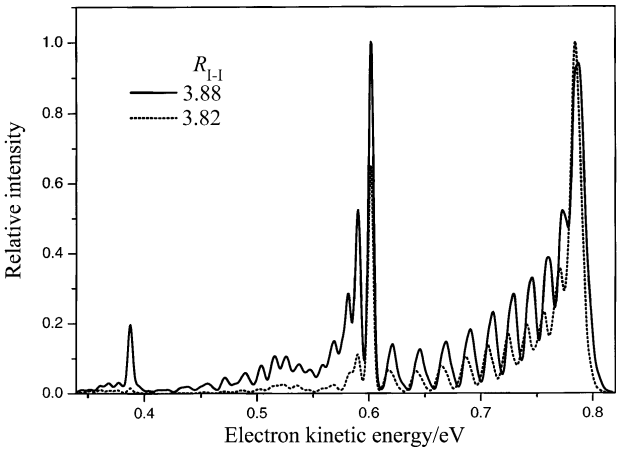

Fig. 8 PE spectrum of IHI^- at interiodine distances of 3.88 and 3.82 Å simulated by the three-dimensional adiabatic method.

$I_2^- \cdot Ar_n$ clusters for $n > 6$, consistent with a stiffer potential and shorter interiodine bond distance induced by clustering with Ar atoms. Taking these other results into account, it appears that at least some of our observed changes in peak spacing can be explained by assuming the interiodine distance in IHI^- is reduced upon clustering to Ar atoms.

There is another possible effect of clustering on the IHI^- geometry suggested by the MD simulations by Parson *et al.*[26] on $I_2^- \cdot Ar_n$ clusters. The simulations indicate that solvation by Ar (or CO_2) distorts the electronic charge distribution of the I_2^-, with more of the excess negative charge localized on the more highly solvated I atom. In $I_2^- \cdot Ar_n$ clusters, these effects are most pronounced around $n = 13$, since for this cluster one of the I atoms is completely solvated and the other is bare (except for the six Ar atoms around the waist of the I_2^- bond). Analogous effects in $IHI^- \cdot Ar_n$ would be particularly interesting, because partial localization of the excess electronic charge on one of the I atoms might be accompanied by loss of $D_{\infty h}$ symmetry of the IHI^- core with unequal H–I bond lengths. This would markedly affect the main ν_3 progression in the PE spectrum, with transitions to neutral levels with odd ν_3' values becoming allowed. We see no obvious evidence of this effect in our PE spectra, suggesting that the interactions with Ar atoms are not strong enough to induce symmetry-breaking of the anion core.

C. Transition state dynamics

The analysis of the previous section showed that changes in the peak spacings of the $IHI^- \cdot Ar_n$ PE spectra could be at least partially explained in terms of perturbation of the anion geometry by the solvent atoms. It is possible that these changes also reflect shifts in the neutral ν_3 level spacing induced by the Ar atoms, but in the light of the above discussion such an interpretation would be quite speculative. Moreover, it is unclear how perturbations by Ar atoms would induce the type of shifts we obseve, with the 0–2 spacing changing while the 2–4 spacing remains constant. One must then consider whether any other effects in these spectra can be more definitively attributed to cluster-induced perturbation of the neutral transition state dynamics.

The theoretical paper by Lavender and McCoy[21] on $ClHCl^- \cdot Ar_n$ provides some guidance on what to look for in the PE spectrum. By means of a time-dependent self-consistent field (TDSCF) calculation, they determine the time-dependent wavefunction for the Cl and H atoms subsequent to photodetachment. Their work shows that clustering has a significant effect on the bending motion of the neutral ClHCl complex. In bare $ClHCl^-$, the initial dynamics involve the H atom rotating off the Cl–Cl axis, *i.e.* the first thing that happens is that the complex leaves its initially collinear configuration. The first five Ar atoms lie in the plane perpendicular to this axis and reduce the configuration space available to the H atom in non-collinear geometries, thereby hindering this bending motion of the H atom. As a consequence, clustering increases the probability

of finding the H atom between the two Cl atoms at early times ($\leqslant$60 fs), and the likelihood for dissociation of the complex to Cl + HCl in near-collinear geometries is also increased.

In order to determine what observable effects might arise from these perturbations of the transition state dynamics, Lavender and McCoy simulated the PE spectra of the clusters. They found that the intensities of the $v'_3 = 0$ and 2 peaks changed upon clustering, with the latter peak becoming less intense with increasing n. In addition, clustering resulted in an observable shoulder on the $v'_3 = 0$ feature that was attributed to enhanced intensity in (unresolved) bend excited states of the neutral complex.

As pointed out in the Results, our PE spectra of $IHI^- \cdot Ar_n$ do show some enhancement of the bend/hindered rotor progression on the $v'_3 = 0$ feature for the largest clusters studied, specifically $n = 11$, 13, and 15 (see Fig. 2). This effect is qualitatively in accord with the calculations of $ClHCl^-$ and is probably our strongest evidence for cluster-induced changes in the transition state dynamics. We do not see any changes in the intensity ratio of the $v'_3 = 0$ and 2 peaks, but it is important to point out that in the PE spectrum of IHI^-, the latter is made up of partially resolved resonances, whereas in the $ClHCl^-$ spectrum both peaks probably result from transitions to repulsive rather than quasi-bound transition state levels.[10] Clearly, this interpretation of our spectra would benefit from further theoretical work on larger clusters of both $ClHCl^-$ and IHI^- with Ar atoms.

D. Isomer

Fig. 4 shows a very weak feature in the $IHI^- \cdot Ar_n$ spectra at around 0.5 eV higher eKE than the main features of the PE spectra in Fig. 2. This high eKE feature is not seen in the bare IHI^- spectrum. Our mass resolution is sufficiently high so that only a single ion mass contributes to each PE spectrum. It therefore appears that the high eKE peak may be due to a structural isomer with the same mass as $IHI^- \cdot Ar_n$.

The vertical detachment energies (VDE) for these isomers are listed in Table 2. Each VDE lies about 0.3 eV above the electron affinity of the corresponding $I^- \cdot Ar_n$ cluster.[32] This comparison suggests that in these clusters, the I^- and HI exist as distinct entities and that the structure of the isomer is $I^- \cdot Ar_n \cdot HI$, possibly a "solvent-separated" structure with one or more Ar atoms lying between the I^- and HI. The mass spectrum in Fig. 1 shows a strong signal from $I^- \cdot Ar_n$ clusters, so attachment of HI to clusters of this type in the free jet expansion could lead to $I^- \cdot Ar_n \cdot HI$ structures. However, these structures would have to survive the transit time through the instrument, of the order of 100 μs, in order to be seen in the PE spectrum, implying a barrier to formation of the more stable $IHI^- \cdot Ar_n$ structure. The overall (highly speculative) picture then is for HI to attach to an $I^- \cdot Ar_n$ cluster and become trapped in a shallow, metastable well as the cluster cools through evaporation of several Ar atoms. Note that isomers of this type were proposed in our earlier study of $IHI^- \cdot (N_2O)_n$ clusters[18] based on evidence similar to that seen here.

Summary

In this paper we have studied the PE spectra of transition state precursors, $IHI^- \cdot Ar_n$. The dependence of the $IHI^- \cdot Ar_n$ PE spectra on the cluster size reflects the solvation effects on both the anion and the neutral transition state complex. The $IHI^- \cdot Ar_n$ PE spectra are similar in form to the bare IHI^- spectrum, but are successively shifted to lower electron kinetic energies. The total shift plot has a distinct reduction in slopes between $n = 0$ to 6 and $n = 7$–15. The stepwise shift also shows a significant drop from $n = 6$ to 7. We have attributed these effects to the binding site change of the argon atoms. The peak spacing between the $v'_3 = 0$ and 2 peaks of the $IHI^- \cdot Ar_n$ spectra is found to be smaller for larger clusters. Based on comparison with three-dimensional adiabatic simulation of the PE spectra, it appears this change is at least in part due to changes in the geometry of the IHI^- anion core in argon clusters. On the other hand, increased intensity in the hindered rotor progressions upon clustering may reflect cluster-induced perturbations of the neutral transition state dynamics. An extra new feature is observed at slightly higher electron kinetic energy. The carrier of this weak feature has been tentatively assigned to an isomer of $IHI^- \cdot Ar_n$ of the form $I^- \cdot Ar_n \cdot HI$.

Further studies of this type are planned with more strongly interacting solvent species such as CO_2 and H_2O. We hope that this series of experiments will yield a more systematic understanding

of the effects of solvation on transition state dynamics, ultimately providing detailed insight into the differences between reaction dynamics in the gas phase and in solution.

Acknowledgements

This research is supported by Air Force Office of Scientific Research under Grant No. F49620-00-1-0145. We thank Professor Ricardo Metz for the help of the three-dimensional adiabatic simulation program.

References

1 M. C. Duval, O. B. Dazy, W. H. Breckenridge, C. Jouvet and B. Soep, *J. Chem. Phys.*, 1986, **85**, 6324.
2 A. H. Zewail, *Science*, 1988, **242**, 1645.
3 P. R. Brooks, *Chem. Rev.*, 1988, **88**, 407.
4 G. C. Schatz, *J. Phys. Chem.*, 1990, **94**, 6157.
5 D. M. Neumark, *Annu. Rev. Phys. Chem.*, 1992, **43**, 153.
6 J. C. Polanyi and A. H. Zewail, *Acc. Chem. Res.*, 1995, **28**, 119.
7 D. M. Neumark, *Acc. Chem. Res.*, 1993, **26**, 33.
8 A. Weaver, R. B. Metz, S. E. Bradforth and D. M. Neumark, *J. Phys. Chem.*, 1988, **92**, 5558.
9 I. M. Waller, T. N. Kitsopoulos and D. M. Neumark, *J. Phys. Chem.*, 1990, **94**, 2240.
10 R. B. Metz, A. Weaver, S. E. Bradforth, T. N. Kitsopoulos and D. M. Neumark, *J. Phys. Chem.*, 1990, **94**, 1377.
11 S. E. Bradforth, A. Weaver, D. W. Arnold, R. B. Metz and D. M. Neumark, *J. Chem. Phys.*, 1990, **92**, 7205.
12 A. Weaver, R. B. Metz, S. E. Bradforth and D. M. Neumark, *J. Chem. Phys.*, 1990, **93**, 5352.
13 D. E. Manolopoulos, K. Stark, H. J. Werner, D. W. Arnold, S. E. Bradforth and D. M. Neumark, *Science*, 1993, **262**, 1852.
14 D. W. Arnold, C. S. Xu and D. M. Neumark, *J. Chem. Phys.*, 1995, **102**, 6088.
15 B. J. Gertner, K. Ando, R. Bianco and J. T. Hynes, *Chem. Phys.*, 1994, **183**, 309.
16 M. Bennun and R. D. Levine, *Int. Rev. Phys. Chem.*, 1995, **14**, 215.
17 M. L. Chabinyc, S. L. Craig, C. K. Regan and J. I. Brauman, *Science*, 1998, **279**, 1882.
18 D. M. Neumark, in *Advances in Molecular Vibrations and Collision Dynamics*, ed. J. M. Brauman and M. A. Ratner, JAI Press, Greenwich, CT, 1991, vol. 1A.
19 D. W. Arnold, PhD Thesis, University of California, Berkeley, 1994.
20 Z. Liu, H. Gomez and D. M. Neumark, *Chem. Phys. Lett.*, 2000, **332**, 65.
21 H. B. Lavender and A. B. McCoy, *J. Phys. Chem. A*, 2000, **104**, 644.
22 K. R. Asmis, T. R. Taylor, C. S. Xu and D. M. Neumark, *J. Chem. Phys.*, 1998, **109**, 4389.
23 J. V. Coe, J. T. Snodgrass, C. B. Freidhoff, K. M. McHugh and K. H. Bowen, *J. Chem. Phys.*, 1987, **87**, 4302.
24 G. Markovich, R. Giniger, M. Levin and O. Cheshnovsky, *J. Chem. Phys.*, 1991, **95**, 9416.
25 D. W. Arnold, S. E. Bradforth, E. H. Kim and D. M. Neumark, *J. Chem. Phys.*, 1995, **102**, 3510.
26 J. Faeder, N. Delaney, P. E. Maslen and R. Parson, *Chem. Phys. Lett.*, 1997, **270**, 196.
27 V. S. Batista and D. F. Coker, *J. Chem. Phys.*, 1999, **110**, 6583.
28 G. N. Vien, N. Rougeau and C. Kubach, *Chem. Phys. Lett.*, 1993, **215**, 35.
29 R. B. Metz and D. M. Neumark, *J. Chem. Phys.*, 1992, **97**, 962.
30 G. C. Schatz, D. Sokolovski and J. N. L. Connor, *Discuss. Faraday Soc.*, 1991, **91**, 17.
31 M. T. Zanni, B. J. Greenblatt and D. M. Neumark, *J. Chem. Phys.*, 1998, **109**, 9648.
32 I. Yourshaw, Y. Zhao and D. M. Neumark, *J. Chem. Phys.*, 1996, **105**, 351.